Surface & Coatings Technology 203 (2008) 490–494

Contents lists available at ScienceDirect

Surface & Coatings Technology

journal homepage: www.elsevier.com/locate/surfcoat

XRD and FTIR analysis of Ti–Si–C–ON coatings for biomedical applications

Cristina Oliveira [a], L. Gonçalves [b], B.G. Almeida [a], C.J. Tavares [a], S. Carvalho [a,*], F. Vaz [a], R. Escobar_Galindo [c], M. Henriques [d], M. Susano [d], R. Oliveira [d]

[a] Universidade do Minho, Dept. Física, Campus de Azurém, 4800-058 Guimarães, Portugal
[b] Universidade do Minho, Dept. de Electrónica Industrial, Campus de Azurém, 4800-058 Guimarães, Portugal
[c] Instituto de Ciencia de Materiales de Madrid (ICMM-CSIC), Cantoblanco, 28049, Madrid, Spain
[d] IBB-Institute for Biotechnology and Bioengineering Centre for Biological Engineering Universidade do Minho Campus de Gualtar, 4700-057, Portugal

ARTICLE INFO

Available online 18 June 2008

Keywords:
Sputtering
FTIR
Resistivity
Biofilm formation

ABSTRACT

Ti–Si–C–ON films were deposited by DC reactive magnetron sputtering using different partial pressure ratio of oxygen (p_{O_2}) and nitrogen (p_{N_2}). Compositional analysis revealed the existence of three different growth zones for the films; (I) N/Ti = 2.1 (high atomic ratio) and low oxygen content; (II) 0.76 < N/Ti < 2.1 (intermediate atomic ratio) and (III) N/Ti ≤ 0.12 (low ratio) and high oxygen content. For high N/Ti atomic ratio (N/Ti = 2.1) the XRD pattern exhibits reflections that correspond to a mixture of two different phases: a metallic-like Ti and a fcc NaCl type structure. Its electrical resistivity presents a metallic character and, consequently, has high infrared reflectivity. For the intermediate N/Ti ratio (0.76 < N/Ti < 2.1), the films crystallize in a B1-NaCl crystal structure typical for $TiC_{0.2}N_{0.8}$. Their FTIR spectra present C–N modes, besides the TiN ones, that indicate a progressive substitution of nitrogen by carbon atoms with increasing oxygen content (and lowering N/Ti ratio). For the highest oxygen content (and lower N/Ti ratio) the presence of the Ti–O–Ti stretching mode shows the formation of highly resistive Ti–O compounds consistent with the semiconductor character of this film. Biofilm formation as well as material cytotoxicity seemed to be related with the presence of the Ti.

1. Introduction

With the advance of technology and the increase in the expectation of life and human development, scientists have intensified their studies in bio-materials science. This made possible the identification of new materials and properties, their limitations and how to manipulate them towards applications. Implant failure is a huge problem for both the patient and government agencies, since it involves repeated surgeries and high costs. This failure can be attributed to excessive wear and wear debris and to microbial infection. The choice of materials to be used as biomaterials requires the analysis and control of a set of properties that must be attained. The effect of the organic environment of the material (corrosion, degradation) and the effect of the material in the organism ("biocompatibility") are phenomena that must be studied with extreme care. In particular, the interaction of living tissues with the biomaterial, associated with the different responses of the organism to its presence, is one of most challenging points in the development of biomaterials. In this regard, the development of wear-resistant biomaterials is far from being completed and the implementation of new multifunctional coatings is a very promising approach to improve the performance of artificial implants.

The purpose of this work is to investigate the feasibility of various Ti–Si–C–ON films for applications in medical devices. Based on known results it is widely accepted that is possible to achieve superhardness by Si incorporation in TiN [1] and a decrease in the Young's modulus is observed by addition of oxygen [2]. The oxygen has always been looked upon as an interesting element in thin film materials, not only because of its high reactivity with most metals, but also due to the changes that it induces in chemical bonding states and, thus, in the materials electrical, optical and mechanical characteristics [3]. In addition, it has been previously shown that the corrosion resistance tends to be slightly improved by oxygen incorporation [4].

Recent work on Ti–Si–C showed that is a promising compound due to its particular structure, as well as its extraordinary mechanical and tribological properties [5]. Taking this into consideration, the main task of this paper is focused on the relationship between the composition, structure, resistivity and the biological behavior, of single-layered TiSiCON films.

2. Experimental details

The Ti–Si–C–ON films were deposited by reactive dc magnetron sputtering in a $Ar+(N_2+O_2)$ atmosphere. Two opposed high purity Ti targets ($20 \times 10\ cm^2$) were used. One with C pieces (TiC target) and the

* Corresponding author. Tel.: + 351 253 510470; fax: + 351 253 510461.
E-mail address: sandra.carvalho@fisica.uminho.pt (S. Carvalho).

0257-8972/$ – see front matter © 2008 Elsevier B.V. All rights reserved.
doi:10.1016/j.surfcoat.2008.06.121

other with Si pieces (TiSi target) embedded in its erosion zone. The films were deposited on silicon, polished stainless steel and polished high-speed steel substrates. The Ar flow was kept constant at 60 sccm. In order to change oxygen and nitrogen ratio on the samples, they were grown with different gas fluxes (the N_2 ranging from 6.5 to 0 sccm, and the O_2 from 0 to 5.25 sccm), which resulted on different ratios of the oxygen and nitrogen partial pressures (p_{O_2}/p_{N_2}). Further information about the film deposition can be found elsewhere [6]. The atomic composition of as-deposited samples was measured by Electron Probe Microanalysis (EPMA) and Glow Discharge Optical Emission Spectroscopy (GDOES). Ball crater tests were used to obtain the thickness of samples. The structure and phase distribution of the coatings were determined by X-ray diffraction (XRD) using a conventional Philips PW 1710 diffractometer, operating with Cu K_α radiation, in a Bragg–Brentano configuration.

Electrical resistivity at room temperature was measured with the Van der Pauw method. The infrared (IR) reflectance of the coatings was measured using a Bruker IFS 66V Fourier Transform Infrared Spectrometer (FTIR). The reflectivity measurements were done at near normal incidence in the spectral range 400–4000 cm^{-1}.

Biofilms of *Staphylococcus epidermidis* were formed on coated materials for 48 h with agitation. Total biomass was determined according to Henriques et al. [7]. Briefly, crystal violet staining was applied on the samples coated with the biofilm (previously washed with phosphate saline solution and fixed with methanol). Staining was removed using 33% acetic acid and the absorbance of the resultant solution was measured at 570 nm. Cytotoxicity was determined by indirect contact of samples with Fibroblasts 3T3 (CCL-163). After 24 h of incubation at 5% CO_2 and 37 °C cellular activity was determined by MTS quantification. The percentage of fibroblasts death was calculated against cell growth in the absence of sample contact (control — 100%).

3. Results and discussion

3.1. Chemical composition

The evolution of the chemical composition of the deposited coatings obtained by the GDOES and EPMA measurements and their correspondent thickness (measured by ball-cratering) is shown in Table 1. It is possible to observe changes in chemical composition as a function of the oxygen partial pressure and the nitrogen partial pressure ratio (p_{O_2}/p_{N_2}). Previously, we have already discussed the changes in chemical composition of the films as a function of deposition process parameters [6]. We leave this matter out of the scope of this paper. Nevertheless, for the sake of clarity some features should be pointed out: the O/Ti and N/Ti ratios in the films do not remain constant, changing as a function of the p_{O_2}/p_{N_2}. The N/Ti atomic ratio has a clear and systematic decrease with increasing p_{O_2}/p_{N_2} and the oxygen content shows an opposite behaviour. A closer look at the N/Ti ratio shows that it can be divided into 3 different regimes: (I) N/Ti = 2.1 (high atomic ratio) and low oxygen content; (II) 0.76 < N/Ti < 2.1 (intermediate atomic ratio), (III) N/Ti ≤ 0.12 (low ratio) and high oxygen content.

These regimes are important for the rest of the discussion since the O content and N/Ti ratio have a competitive role on the film properties.

3.2. Phase composition

In order to understand the mechanism of structure evolution with variation of p_{O_2}/p_{N_2} (and consequently with the N/Ti atomic ratio in the films), XRD analysis was carried out. Fig. 1 shows the XRD diffraction patterns for the deposited samples with different N/Ti atomic ratios. The reference peaks, obtained from International Centre for Diffraction Data (ICDD) database, for the materials α-Ti (ICDD card nr. 44-1294), TiN (ICDD card nr. 38-1420, TiC (ICDD card nr. 01-071-6256), and $TiC_{0.2}N_{0.8}$ (ICDD card nr. 01-076-2484) are also included at the top of Fig. 1. The differences in the composition are well correlated with the differences observed in the developed structure. In fact from the diffraction patterns it is possible to observe three different behaviors in agreement with the N/Ti regimes described before.

The XRD pattern from the samples with high N/Ti atomic ratio (N/Ti = 2.1) exhibits reflections that correspond to a mixture of two different phases: a metallic-like Ti and an fcc NaCl type structure. The $2\theta \approx 38.6°$ peak can be attributed to a Ti phase (probably due the interlayer), since the position is close to the (002) of α-Ti, which is known to be the typical orientation of sputtered Ti coatings [8]. The other peaks match with a fcc TiN phase. These peaks move to lower angles (comparing with the stress free TiN lattice) with decreasing N/Ti, due to a gradual substitution of nitrogen atoms by carbon atoms in the TiN structure [9]. Other diffraction peaks from crystalline phase such SiN_x, SiC, phases were not detected, if existent they are probably in an amorphous phase.

For the intermediate N/Ti ratio (0.76 < N/Ti < 2.1), the films crystallize also in a B1-NaCl crystal structure typical for $TiC_{0.2}N_{0.8}$. The sample with N/Ti = 0.8 shows an additional diffraction peak, at 44.6°, which can be assigned to the (101) direction of $Ti_2C_{0.06}$ with hexagonal structure, in accordance with the ICDD card number 051-0628. However, it is difficult to unequivocally identify which phases are formed. E.V. Shalaeva et al. [10] stated that for Ti–Si–N–O films a silicon content of 10 at.% induced a nearly single-phase crystalline structure of TiSiN(O) with minimum grain size 1.5–2 nm. In our case, the diffraction analysis does not allow to conclude that silicon is partially dissolved in a cubic solid solution of TiSiN(O). Carbon and oxygen substitution of regular nitrogen positions to form an fcc Ti(C,O,N) phase, once the nitrogen content decreases and oxygen increases, can also be possible. A.C. Fernandes et al. suggest that for TiC_xO_y films, due the high chemical affinity of Ti to O, this element may be incorporated into the TiC films during deposition forming a Ti–C–O solid solution [11].

The films grow with a preferred (111) orientation that is progressively enhanced with decreasing N/Ti ration. The texture evolution can be related with the decrease on the Nitrogen content, as described in [12]. However, by increasing the oxygen flow (increasing the p_{O_2}/p_{N_2} ratio) the oxygen behaviour is not linear. For lower flow rates, dissociation of the oxygen molecules can occur, which increases the reactivity of the system and thus the deposition rate. An increase

Table 1
Chemical composition, deposition parameters, electrical and biological properties of the deposited samples

Sample	p_{O_2}/p_{N_2}	Chemical composition					Thickness (μm)	Deposition rate (μm/h)	Ratio N/Ti	Resistivity (Ω m)	Abs CV	% cell death
		Ti (at.%)	Si (at.%)	C (at.%)	O (at.%)	N (at.%)						
A	0.046	26.1	10.28	6.4	2.9	54.9	1.4	0.93	2.1	4.39121E−06	0.22	8
B	0.56	26.3	7.5	2.9	14.5	48.7	1.7	1.1	1.85	9.82661E−06	0.33	13
C	0.6	25.0	7.9	3.8	16.5	46.2	1.8	1.2	1.84	1.6681E−05	0.25	7
D	0.8	40.9	7.1	9.3	10.9	31.4	1.83	1.2	0.8	6.4705E−06	0.25	22
E	1.76	58.0	7.82	9.75	17.4	7.0	2.2	1.46	0.12	2.07455E−06	0.17	35
F	20	54.4	4.5	3.3	34.7	2.1	2.4	1.6	0.04	69260.7	0.22	–

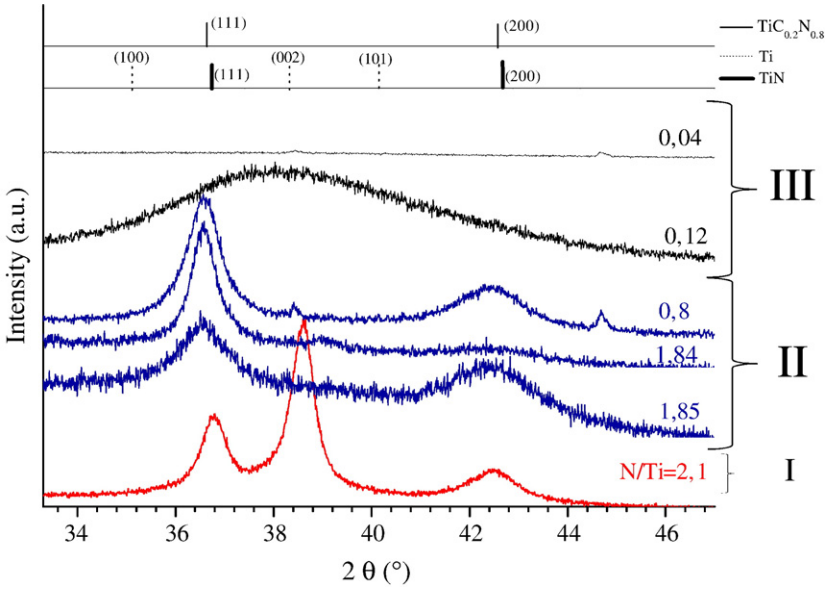

Fig. 1. XRD patterns of the TiSiCON coatings deposited by DC reactive magnetron sputtering, with different of the N/Ti ratios.

on the deposition rate without a significant increase in the bias current density implies a decrease in the adatom mobility. Then, it is very common to have thin films with (111) fcc-type oriented structures, when using low adatom mobility [13].

The samples deposited with high p_{O_2}/p_{N_2}, that induces a low N/Ti atomic ratio and a high oxygen content (regime N/Ti ≤ 0.12), exhibit a polycrystalline structure, with formation of nanosized clusters. For the N/Ti = 0.12 sample the structure is only characterized by a very broad peak in the range 30 to 50°, centered at $2\theta = 37.9°$, which is not enough to identify the structure. However, there are fcc phases that have the main peaks close this values (Ti–O, Ti–Si–N, Ti–C–N, Ti–C–O–N, Ti–C–O, Ti–Si (O)N, Ti–O–N) [13–17]. On the other hand, by increasing the p_{O_2}/p_{N_2} ratio and, consequently, the increase of the oxygen concentration, the increasing content of N-vacancies (decreasing N/Ti) can progressively be filled by oxygen atoms.

3.3. IR-reflectance and electrical properties

In order to further access the chemical composition of the samples and, in particular identify the chemical bonding of the species that were not directly evident from the XRD results, FTIR measurements were performed on the samples. Fig. 2 shows the infrared reflectivity spectra of the films. For low oxygen concentration the infrared reflectivity is high, attaining values above 80% for wave-numbers near 1000 cm^{-1}. As the O content increases the reflectivity strongly decreases, so that for the sample with higher oxygen concentration (34.7%) several bands are present on the IR spectrum.

The high reflectivity values of the samples with low O content (and high and intermediate N/Ti ratio), as well as the monotonous behavior of their corresponding spectra are due to the metallic character of these films. In fact, they present electrical resistivities in the range

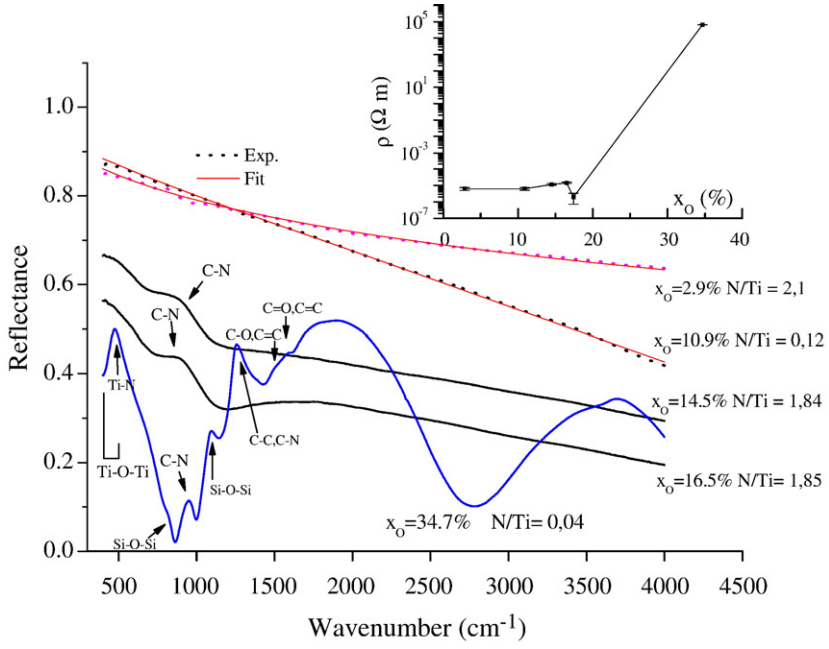

Fig. 2. Infrared reflectivity spectra of the TiSiCON coatings for different oxygen concentrations x_O (or N/Ti ratios). The inset shows the corresponding electrical resistivity of the films. The fit to the curves with 2.9% and 10.9% oxygen concentrations was performed by using Eq. (1) in the text.

6×10^{-2}–10×10^{-2} Ω m ($x_O<17\%$, N/Ti>0.8), as shown in the inset of Fig. 2. These values are slightly higher than that found on TiN (<2×10^{-2} Ω m [18]) However, nitrogen substitution by carbon atoms, to form fcc Ti(C,N) phases as discussed on the XRD results, induces an increase on the electrical resistivity, in agreement with what was found on $TiC_{0.5}N_{0.5}$ coatings [19].

As the oxygen concentration increases and the N/Ti ratio decreases, the electrical resistivity of the films increases, attaining 6.6×10^4 Ω m for the sample with higher oxygen content (34.7%). The value measured on this sample is characteristic of a semiconductor. Since the increase of oxygen concentration in the films promotes the formation of nanosized clusters (grain sizes from 9 to 4 nm), as observed from the broadening on the XRD peaks of Fig. 1, this induces an increase of the grain boundary scattering contribution to the electrical resistivity of the films. Additionally, the decrease of the N/Ti ration and the increase of the O content induces the formation of Ti–O residual phases which have very high electrical resistivities. Both effects then combine to the overall increase of the resistivity of the films, and, in particular, to the change to a semiconductor character of the film with higher oxygen content.

The high reflectivity of the low oxygen concentration can be simply modeled using a complex dielectric function with a plasmon term [20,21], which takes into account the presence of free charges (ie. the finite conductivity of the film). Accordingly:

$$\varepsilon_{\text{film}}(\omega) = \varepsilon_{\infty p} - \frac{\omega_p^2}{\omega^2 + i\gamma_p\omega} \quad (1)$$

where $\omega_p^2 = 4\pi Ne^2/m^*$ represents the bulk plasma frequency due to free carriers of density N and effective mass m^*. γ_p is the free-carrier damping constant and e is the electron charge. For the films used $m^* = m_e$ (m_e being the electron mass). The infrared reflectivity of the films can then be determined by [20]:

$$R = \left|\frac{1-n}{1+n}\right| \quad (2)$$

where $n = \sqrt{\varepsilon}$ is the complex refraction index and ε is the complex dielectric constant of Eq. (1). Fig. 2 shows the fittings results obtained for the samples with oxygen concentrations of 2.87% and 0.89%. The obtained plasma frequencies for the particular films shown were 51,100 cm^{-1} and 11,610 cm^{-1}. These values correspond to a carrier density of 2.72×10^{21} cm^{-3} and 6.19×10^{20} cm^{-3}, respectively.

The above model cannot be applied so simply to the samples with higher oxygen content, due to the decreasing resistivity of the films and the progressive appearance of bands corresponding to the characteristic vibrations of the bonds between the species composing the samples. Instead, we have opted to identify them based on the frequencies of the observed bands. For the sample with higher resistivity (higher oxygen content and lower N/Ti ratio), the vibrations that were ascribed to the observed bands are summarized in Table 2.

The Ti–N and Ti–O–Ti bands at lower wavenumbers are overlapped. However, for low oxygen concentrations (and high N/Ti content) the broad band below ~600 cm^{-1} corresponds mainly to vibration mode from TiN since it was this phase that was found to be dominant on the XRD results, for the low O concentration region. On the other hand, for the high oxygen (and low N/Ti ratio) sample the band becomes more sharply defined due to the additional presence of the Ti–O–Ti stretching vibration mode and, consequently, to formation of high resistivity Ti–O residual compounds on this sample. The presence of additional Si–O–Si characteristic modes on this film corresponds to SiO_x compounds that form on top of the silicon substrates when they are exposed to the background reactive atmosphere, on the deposition chamber.

The appearance of the C–N modes on the intermediate N/Ti ratio (or intermediate O content) samples is consistent with the progressive substitution of the nitrogen by carbon on the underlying TiN structure, as discussed on the previous XRD results of Fig. 1. The small bands above 1500 cm^{-1} show the presence of C–O, C═O and C═C bonds, but their small intensity indicates that the sample presents a small amount of these bonds.

Table 2
Bands observed on the infrared spectra of the Ti–Si–C–ON coatings and the correspondingly assigned vibration modes

Wavenumber (cm−1)	Assignment	Reference
400–500	Ti–O–Ti	[22]
~480	TiN	[23]
~800	Si–O symmetric stretching	[22]
~900, 1050	C–N Waggling and C–N (sp^3 hybridization)	[24]
~1000–1200	Si–O asymmetric stretching	[22]
1200–1700	C═N stretching and aromatic C═C stretch	[24]
1245, 1300–1270	C–C sp^2/sp^3	[24]
1445	C–O	[25]
1647	C═O	[26]

3.4. Biological properties

The Abs CV results (Table 1) showed that *S. epidermidis* 1942 was able to form biofilms on all samples, but independently of the surface physical properties assayed. Concerning cytotoxicity (Table 1), overall, samples present low values of cell death (<35%), however, samples with N/Ti ≥ 1.84 have significantly lower values of cytotoxicity than the other two samples analyzed. It must be stressed out that cytotoxicity of sample with the lowest N/Ti atomic ratio was not determined once it was damaged.

Moreover, biofilm formation as well as material cytotoxicity seemed to be related with surface chemical composition, namely, with the presence of Ti. It is interesting to note that the sample with N/Ti = 0.12, with the highest cytotoxicity, is the less prone to *S. epidermidis* biofilm formation, stressing the importance of joining both biological assays: biofilm formation and cytotoxicity, to evaluate biocompatibility.

4. Conclusions

Ti–Si–C–ON thin films were deposited by reactive magnetron sputtering with different p_{O_2}/p_{N_2}. The results show that O content and N/Ti ratio have a competitive role on the film properties. The FTIR results show that for low oxygen concentrations (and high N/Ti content) a band below ~600 cm^{-1} corresponds mainly to vibration mode from TiN, since it was this phase that was found to be dominant on the XRD results. On the other hand, for the sample with highest oxygen content (and lower N/Ti ratio) the band becomes more sharply defined due to the additional presence of Ti–O–Ti stretching vibration mode and, consequently, to formation of highly resistivity Ti–O compounds on the film. Biofilm formation as well as material cytotoxicity seemed to be related with surface chemical composition, namely, with the presence of Ti.

References

[1] S. Veprřek, A. Nioderhofer, K. Moto, et al., Surf. Coat. Technol. 133–134 (2000) 152.
[2] F. Vaz, P. Cerqueira, L. Rebouta, S.M.C. Nascimento, E. Alves, Ph. Goudeau, J.P. Rivière, Surf. Coat. Technol. 174–175 (2003) 197.
[3] A.C. Fernandes, P. Carvalho, F. Vaz, S. Lanceros-Méndez, A.V. Machado, N.M.G. Parreira, J.F. Pierson, N. Martin, Thin Solid Films 515 (2006) 866.
[4] E. Ariza, L.A. Rocha, F. Vaz, L. Cunha, S.C. Ferreira, P. Carvalho, L. Rebouta, E. alves, Ph. Goudeau, J.P. Rivière, Thin Solid Films 469–470 (2004) 274.
[5] C. Lopes, N.M.G. Parreira, S. Carvalho, A. Cavaleiro, J.P. Rivière, E. Le Bourhis, F. Vaz, Surf. Coat. Technol. 201 (2007) 7180.
[6] Freddy Guimarães, Cristina Oliveira, Elsa Sequeiros, Marta Torres, M. Susano, M. Henrique, R. Oliveira, R. Escobar Galindo, S. Carvalho, N.M.G. Parreira, F. Vaz, A. Cavaleiro, Surf. Coat. Technol. 202 (2008) 2403.

[7] M. Henriques, J. Azeredo, R. Oliveira, Br. J. Biomed. Sci. 63 (2006) 5.
[8] Vaz, J. Ferreira, E. Ribeiro, L. Rebouta, S. Lanceros-Méndez, J.A. Mendes, F. Ribeiro, I. Moutinho, Ph. Goudeau, J.P. Rivière, E. Alves, K. Pischow, J. de Rijk, Surf. Coat. Technol. 191 (2005) 317.
[9] S.W. Huanga, M.W. Ng, M. Samandi, M. Brandt, Wear 252 (2002) 566–579.
[10] E.V. Shalaeva, S.V. Borisov, O.F. Denisov, M.V. Kuznetsov, Thin Solid Films 339 (1999) 129.
[11] A.C. Fernandes, F. Vaz, L. Rebouta, A. Pinto, E. Alves, N.M.G. Parrreira, Ph. Goudeau, E. Le Bourhis, J.P. Rivière, Surf. Coat. Technol. 201 (2007) 5587.
[12] C. Moura, P. Carvalho, F. Vaz, L. Cunha, E. Alves, Thin Solid Films 515 (2006) 1132.
[13] S. Carvalho, L. Rebouta, A. Cavaleiro, L.A. Rocha, J. Gomes, E. Alves, Thin Solid Films 398–399 (2001) 391.
[14] E. Ribeiro, L. Rebouta, S. Carvalho, F. Vaz, G.G. Fuentes, R. Rodriguez, M. Zazpe, E. Alves, Ph. Goudeau, J.P. Rivière, Surf. Coat. Technol. 188–189 (2004) 351.
[15] D.V. Shtansky, E.A. Levashov, N.A. Glushankova, N.B. D'yakonova, S.A. Kulinich, M.I. Petrzhik, F.V. Kiryukhantsev-Korneev, F. Rossi, Surf. Coat. Technol. 182 (2004) 101.
[16] Jun-Ha Jeon, Sung Ryong Choi, Won Sub Chung, Kwang Ho Kim, Surf. Coat. Technol. 188–189 (2004) 415.
[17] F. Vaz, P. Cerqueira, L. Rebouta, S.M.C. Nascimento, E. Alves, Ph. Goudeau, J.P. Rivière, K. Pischow, J. de Rijk, Thin Solid Films 447–448 (2004) 449–454.
[18] F. Vaz, P. Machado, L. Rebouta, J.A. Mendes, S. Lanceros-Méndez, L. Cunha, S.M.C. Nascimento, Thin Solid Films 420–421 (2002) 421.
[19] J. Kozlowski, J. Markwski, A. Prajzner, J. Zdanowski, Surf. Coat. Technol. 98 (1998) 1440.
[20] E.D. Palik, Handbook of Optical Constants of Solids, Academic Press, New York, 1985.
[21] B.G. Almeida, A. Pietka, P. Caldelas, J.A. Mendes, J.L. Ribeiro, Thin Solid Films 513 (2006) 275.
[22] S. Permpoon, M. Houmard, D. Riassetto, L. Rapenne, G. Berthomé, B. Baroux, J.C. Joud, M. Langlet, Thin Solid Films 516 (2008) 957–966.
[23] L.I. Wei, Jun-Fang Chen, Appl. Surf. Sci. 253 (2007) 7019.
[24] I.V. Afanasyev-Charkin, M. Nastasi, Surf. Coat. Technol. 186 (2004) 108.
[25] J. García, T. López, M. Álvarez, D.H. Aguilar, P. Quintana, J. Non-Cryst. Solids 354 (2008) 729.
[26] Xiaoyun Ye, Yuming Zhou, Jing Chen, Yanqing Sun, Mater. Chem. Phys. 106 (2007) 447.